Current Research in Toxicology 6 (2024) 100164

Contents lists available at ScienceDirect

Current Research in Toxicology

journal homepage: www.journals.elsevier.com/current-research-in-toxicology

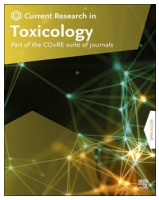

Investigation of *in vitro* biotransformation of tris (1-chloro-2-propyl) phosphate and confirmation in human urine

Fatima den Ouden [a,*], Andrea Estévez-Danta [b], Lidia Belova [a], Celine Gys [a], Anna Klimowska [a,c], Maarten Roggeman [a], Natan Van Wichelen [a], José Benito Quintana [b], Rosario Rodil [b], Giulia Poma [a], Adrian Covaci [a,*]

[a] *Toxicological Centre, University of Antwerp, 2610 Wilrijk, Belgium*
[b] *Department of Analytical Chemistry, Nutrition and Food Chemistry. Institute of Research on Chemical and Biological Analysis (IAQBUS), Universidade de Santiago de Compostela, 15782 Santiago de Compostela, Spain*
[c] *Department of Toxicology, Faculty of Pharmacy, Medical University of Gdańsk, Gdańsk, Poland*

ARTICLE INFO

Keywords:
TCIPP
In vitro metabolism
Human liver microsomes
Human liver cytosol
In vivo metabolism
Human exposome

ABSTRACT

Tris (1-chloro-2-propyl) phosphate (TCIPP) is one of the major organophosphate flame retardants present in the indoor and outdoor environment. Knowledge of biotransformation pathways is important to elucidate potential bioavailability and toxicity of TCIPP and to identify relevant biomarkers. This study aimed to identify TCIPP metabolites through *in vitro* human metabolism assays and finally to confirm these findings in urine samples from an occupationally exposed population to propose new biomarkers to accurately monitor exposure to TCIPP.

TCIPP was incubated with human liver microsomes and human liver cytosol to identify Phase I and Phase II metabolites, by liquid chromatography coupled to quadrupole time-of-flight mass spectrometry (LC-QTOF-MS). Using a suspect-screening approach, the established biomarkers bis (1-chloro-2-propyl) hydrogen phosphate (BCIPP) and 1-hydroxy-2-propyl bis (1-chloro-2-propyl) phosphate (BCIPHIPP) were identified. In addition, carboxyethyl bis (1-chloro-2-propyl) phosphate (TCIPP-M1), bis (1-chloropropan-2-yl) (-oxopropan-2-yl) phosphate (TCIPP-M2) and 1-chloro-3-hydroxypropan-2-yl bis (1-chloropropan-2-yl) phosphate (TCIPP-M3) were identified. TCIPP-M2, an intermediate product, was not reported before in literature. In urine samples, apart from BCIPP and BCIPHIPP, TCIPP-M1 and TCIPP-M3 were identified for the first time. Interestingly, BCIPP showed the lowest detection frequency, likely due to the poor sensitivity for this compound. Therefore, TCIPP-M1 and TCIPP-M3 could serve as potential additional biomarkers to more efficiently monitor TCIPP exposure in humans.

1. Introduction

Flame retardants (FRs) are chemicals added to textiles, plastics, furniture, electronic devices and other consumer goods to reduce the risk of fire spreading and adhere to flammability standards. Since the ban on polybrominated diphenyl ethers (PBDEs), a specific subgroup of brominated flame retardants (BFRs), the class of organophosphate flame retardants (PFRs) is increasingly used (van der Veen & de Boer, 2012; European Chemicals Agency, 2023). The European Chemicals Agency (ECHA) reports a worldwide consumption of FRs of more than 2.4 million tons in 2019, of which 18 % comprises PFRs (European Chemicals Agency, 2023). Moreover, the consumption of FRs will keep increasing with the growth of the global economy (European Chemicals Agency, 2023).

Halogenated PFRs, such as tris (2-chloro-1-(chloromethyl)ethyl) phosphate (TDCP) and tris (1-chloro-2-propyl) phosphate (TCIPP), are used as FRs e.g. in polyurethane, while the non-halogenated PFRs, e.g. triphenyl phosphate (TPHP), are added as flame retardant plasticizers predominantly in flexible PVC (van der Veen & de Boer, 2012). Since PFRs are not chemically bound to materials, they can be released into different environments through volatilization, leaching or abrasion (van der Veen and de Boer, 2012; Wei et al., 2015). The degree of volatilization and leaching is dependent on the substance properties and the matrix into which the substance is incorporated (Schwope et al., 1990; Piringer & Baner, 2008).

TCIPP is applied in polymers such as polyurethane foams (PUFs),

* Corresponding authors.
E-mail addresses: fatima.denouden@uantwerpen.be (F. den Ouden), adrian.covaci@uantwerpen.be (A. Covaci).

https://doi.org/10.1016/j.crtox.2024.100164
Received 13 December 2023; Received in revised form 14 March 2024; Accepted 19 March 2024
Available online 20 March 2024

plastics and coatings (Hammel et al., 2017; European Chemicals Agency, 2023) and is one of the major PFRs present in the indoor and outdoor environment (van der Veen & de Boer, 2012; Blum et al., 2019). Humans can be exposed to TCIPP mostly via diet or inadvertent dust ingestion/inhalation (Hou et al., 2016). In addition, the higher volatility of TCIPP (vapor pressure of 5.64×10^{-5} mmHg) compared to other PFRs might lead to a higher potential for human exposure through inhalation of contaminated air (Hou et al., 2016; Estill et al., 2019). TCIPP has been widely reported in different matrices including dust (Araki et al., 2014; Christia et al., 2019; de la Torre et al., 2020), food (Poma et al., 2017; Poma et al., 2018; Gbadamosi et al., 2022), human blood (Hou et al., 2020; Li et al., 2020; Hou et al., 2021), breast milk (Beser et al., 2019; Chen et al., 2021) and human hair (Liu et al., 2016; He et al., 2018).

While TCIPP and other PFRs are generally considered as a safer alternative for the banned BFRs, there is evidence suggesting that PFRs may also have hazardous properties (Blum et al., 2019). TCIPP has been shown to negatively impact the development of chicken embryos (Farhat et al., 2013) and it was shown to have a toxic effect on human cell lines (Li et al., 2017). In addition, TCIPP is classified as a suspected carcinogen by the World Health Organisation (EHC, 1998) and its chemical structural similarity to the cancer-causing TCEP and TDCIPP raises concerns (OEHHA, 2021). In an ECHA screening report, TCIPP was identified among other chlorinated trialkyl phosphates as a risk for children when they are exposed to flexible PUFs in childcare articles and residential upholstered furniture (European Chemicals Agency, 2018). Furthermore, a recent report of the National Toxicology Program of the US Department of Health and Human Services concluded that there was 'some evidence' of carcinogenic activity in male rats, female rats and male mice, while in female mice 'clear evidence' of carcinogenic activity was found (NTP, 2023). In epidemiological studies in humans, associations between TCIPP concentrations in dust and the occurrence of atopic dermatitis were found (Araki et al., 2014), while in another study, positive associations between the concentrations of TCIPP metabolites and rhino-conjunctivitis were found (Araki et al., 2018).

Knowledge of biotransformation pathways is important to elucidate potential bioavailability and toxicity of TCIPP and to identify potentially useful biomarkers. Bis (1-chloro-2-propyl) hydrogen phosphate (BCIPP) and 1-hydroxy-2-propyl bis (1-chloro-2-propyl) phosphate (BCIPHIPP), two established metabolites of TCIPP, have been identified as biomarkers of TCIPP exposure in urine in multiple studies (Hammel et al., 2016; Bastiaensen et al., 2018; Luo et al., 2021). In addition to these two metabolites, *in vitro* studies identified two other TCIPP Phase I metabolites: carboxyethyl bis (1-chloro-2-propyl) phosphate (TCIPP-M1) (Abdallah et al., 2015; Van den Eede et al., 2016) and 1-chloro-3-hydroxypropan-2-yl bis (1-chloropropan-2-yl) phosphate (TCIPP-M3) (Van den Eede et al., 2016; Wan et al., 2017). However, these two metabolites have not yet been reported in human urine. *In vitro* identification of additional metabolites and their further confirmation in urine could help contribute to a more accurate biomonitoring of exposure to TCIPP.

Therefore, this study aimed to first identify TCIPP metabolites *in vitro* using human liver microsomes (HLMs) and human liver cytosol (HLCYT) to produce Phase I and Phase II metabolites. Subsequently, it aimed to confirm the presence of these metabolites in urine samples from an occupationally exposed population using a suspect screening approach with the ultimate goal to propose additional potential biomarkers for future biomonitoring of TCIPP.

2. Materials and methods

Details about chemicals and reagents can be found in the supplementary information section SI-1.

2.1. In vitro metabolism assay

The *in vitro* assay used in this study was optimized based on a previously described approach (Gys et al., 2018; Vervliet et al., 2020). The experimental set-up is displayed in Fig. 1. All sample sets (Phase I 1 h, Phase I 3 h, Phase II glucuronidation and Phase II sulfation) consisted of three replicates.

Phase I metabolites were generated using HLMs (20 mg/mL, pooled, mixed gender, n = 200 (Xenotech, Kansas City, USA)). A reaction mixture consisting of 955 μL (or 935 μL depending on if the sample was a control, Phase I or Phase II sample) Tris buffer, 25 μL HLM solution (20 mg/mL) and 10 μL TCIPP solution (0.5 mM in DMSO) was incubated in an Eppendorf tube at 37 °C for 1 or 3 h. After 5, 60 and 120 min of incubation, 10 μL of NADPH solution (0.1 M in Tris buffer) was added. After 1 or 3 h, the reaction was stopped using 250 μL of ice-cold acetonitrile (ACN) containing 1 % formic acid and 5 μg/mL of the internal standards (IS) DPHP-d10 and TCEP-d12. Since no deuterated TCIPP was available, internal standards of PFRs structurally similar to TCIPP and its metabolites were used. After vortexing, the samples were centrifuged for 5 min at 8000 rpm (5867 g). The supernatant was transferred to a glass tube, evaporated until near dryness under a gentle nitrogen stream (37 °C) and reconstituted in 100 μL of methanol MeOH: H_2O (1:1; *v/v*). Finally, samples were filtered (0.2 μm nylon, VWR, Leuven, Belgium) in a micro-centrifuge at 8000 rpm (5867 g) and transferred to vials for LC-QTOF-MS analysis.

Three negative controls (either without TCIPP, without HLMs or without cofactor) were prepared in parallel. For Phase I biotransformation, a positive control was prepared by using phenacetin (10 μL of 5 μg/mL in ultrapure water) as a substrate. Formation of two established Phase I biotransformation products of phenacetin, N-(4-hydroxyphenyl)-acetamide (phenacetin-M1) and N-(4-ethoxy-2-hydroxyphenyl)-acetamide (phenacetin-M2), were monitored (Hinson, 1983; Christia et al., 2021).

For formation of Phase II metabolites, samples were subjected to Phase II conjugation via glucuronidation (GLU) or sulfation (SUL) following the Phase I experiments. In this case, the Phase I samples were centrifuged at 8000 rpm (5867 g) for 5 min after 3 h of incubation.

For glucuronidation, 935 μL supernatant originating from the Phase I samples was incubated for 3 h with 25 μL HLMs (20 mg/mL) and 10 μL of alamethicin solution (1 mg/mL in DMSO) at 37 °C. After 5, 60 and 120 min of incubation, 10 μL of UDPGA (100 mM in Tris buffer) was added.

For sulfation, 965 μL supernatant originating from the Phase I samples was incubated with 25 μL HLCYT (10 mg/mL, pooled, mixed gender, n = 50 (Xenotech, Kansas City, USA)) at 37 °C for 3 h. After 5, 60 and 120 min of incubation, 10 μL of PAPS (10 mM in Tris buffer) was added. The Phase II reactions were stopped after 3 h in the same way as described for the Phase I reactions. Samples that did not go through prior Phase I biotransformation were added to the Phase II experiments.

Negative controls for Phase II biotransformation consisted of samples without adding co-factor and samples without adding TCIPP. The positive control was prepared by using 4-nitrophenol (10 mM in Tris buffer) and monitoring the established Phase II biotransformation products 4-nitrophenol glucuronide and 4-nitrophenol sulfate (Tukey & Strassburg, 2000; Gamage et al., 2006). The volume of organic solvent did not exceed 1 % during the incubation to avoid any effect on the microsomal activity (Jia et al., 2007).

2.2. Urine samples

Urine samples (n = 56) were obtained from workers occupationally exposed to TCIPP before and after their shift and collected in polypropylene cups. After shipment, samples were stored at −18 °C. Workers were informed about the details of the study by their Environmental Health and Safety managers and participating workers gave informed consent to voluntarily donate urine samples. In addition, nine control samples were obtained from people working on factory grounds but not in direct contact with TCIPP (e.g. administrative workers).

Samples, quality controls and blanks were extracted using solid phase extraction (SPE) as described by (Bastiaensen et al., 2018). Of

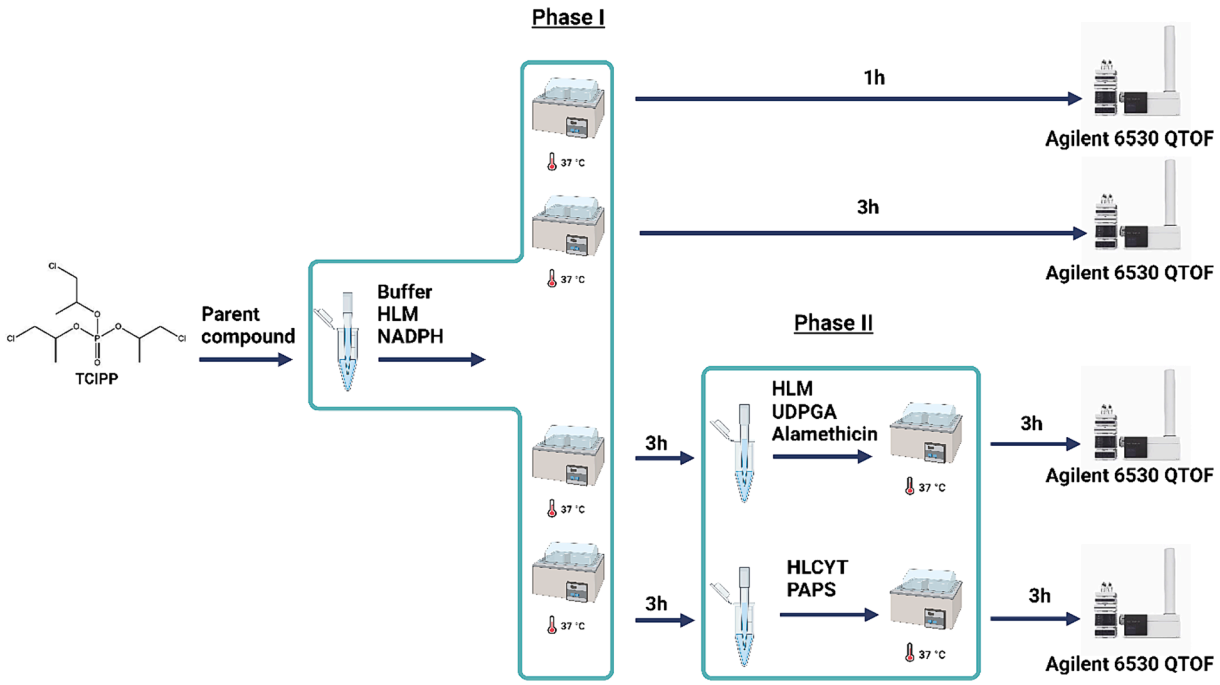

Fig. 1. Overview of the experimental set-up of the *in vitro* metabolism assay used in this study. Created with BioRender.com.

each sample, 1 mL was spiked with 5 ng of mass-labeled internal standard solution (DPHP-d10 and TCEP-d12), adjusted to pH 6 with phosphate buffer and deconjugated with β-glucuronidase (2 mg/mL) during a 2 h incubation at 37 °C. Sample extraction was done on Bond-Elut C18 cartridges (3 mL, 200 mg, Agilent, Santa Clara, USA) conditioned with 3 mL of MeOH followed by 2 mL of ultrapure water. Analytes were eluted with 3 mL MeOH, evaporated until near dryness and reconstituted in 150 μL MeOH:H_2O (1:1; *v/v*).

Extracts were first injected on an Agilent 1290 Infinity II liquid chromatography (LC) system coupled to a triple quadrupole mass spectrometer (ESI-6495) for targeted analysis to identify the samples with the highest concentrations of the TCIPP metabolites BCIPP and BCIPHIPP using a previously validated method (Bastiaensen et al., 2018). Separation was achieved on a Kinetex Biphenyl column (2.1 mm × 100 mm, 2.6 μm particle size, Phenomenex, Torrance, USA) using 5 mM ammonium acetate in ultrapure water with 2 % MeOH as mobile phase A and 5 mM ammonium acetate in MeOH with 2 % ultrapure water as mobile phase B. The instrument was operated in dynamic multiple reaction monitoring in positive and negative ionization mode. Samples showing the highest concentrations of BCIPP and BCIPHIPP, blanks and quality controls were then selected for suspect screening on the LC-QTOF-MS as described in section 2.3.

2.3. LC-QTOF-MS analytical method

Extracts (both *in vitro* and urine samples) were analyzed on an Agilent 1290 Infinity LC coupled to an Agilent 6530 QTOF (Agilent, Santa Clara, CA, USA). Chromatographic separation was achieved using a Kinetex Biphenyl column (2.1 mm × 100 mm, 2.6 μm particle size, Phenomenex, Torrance, USA). The mobile phase consisted of 5 mM ammonium acetate in ultrapure water with 2 % MeOH (A) and 5 mM ammonium acetate in MeOH with 2 % ultrapure water (B). The flow was set at 0.350 mL/min, the injection volume was 5 μL and the column temperature was set at 35 °C. All samples were analyzed in both positive and negative ionization mode. Chromatographic conditions were the same for both polarities. The run started with 5 % B for 0.5 min, then B was increased to 50 % over a time span of 5 min. In the next 4 min, B was increased to 65 % followed by an increase to 99 % B over the next 5 min. This was kept for 4 min, then B decreased to 5 % in 0.1 min. The %B was then kept at 5 % for the remaining 2.4 min of the run. For both polarities the instrument was operated in the 2 GHz (extended dynamic range) mode. The ions with *m/z* 121.0508 and 922.0097 for positive mode and *m/z* 119.0363 and 980.0163 for negative mode, originating from a constantly infused reference mass solution, were selected for constant mass calibration during the chromatographic run to ensure high mass accuracy.

Settings of the Agilent Jet Stream electrospray ionization (AJS-ESI) were as follows: drying gas temperature and flow were 325 °C and 11 L/min (N_2), respectively. Sheath gas temperature was 275 °C with a sheath gas flow of 11 L/min (N_2). Nebulizer pressure was kept at 30 psi. Capillary, nozzle and fragmentor voltages were 3500 V, 0 V and 120 V, respectively. Acquisition parameters for the *m/z* range were set from 50 to 1000 at a scan rate of 4 spectra/s for MS and 8 spectra/s for MS/MS spectra. Collision energies were applied at 10, 20 and 40 eV. Signals were detected using data-dependent acquisition mode (Auto MS/MS) with an isolation width of 4.0 amu. An active exclusion of 0.10 min was applied to prevent repetitive acquisition of MS/MS spectra for the same ion. Data was stored in centroid mode. For urine samples, additional injections in targeted MS/MS mode using selected precursor ions were performed to obtain fragmentation spectra of metabolites.

2.4. Data analysis

Analysis of the acquired data was done using a suspect screening approach. A suspect list was created combining results from *in silico* predictions using Meteor Nexus software 2.4 (Lhasa Limited, Leeds, UK) and a literature search. The generated list of 27 possible biotransformation products of TCIPP, containing their molecular formulae, exact mass, retention time (if available) and a potential name, was exported as a CSV file.

This suspect list was used to detect predicted biotransformation products in the samples using the Targeted Feature Extraction algorithm in MassHunter Profinder 10.0 (Agilent Technologies, Santa Clara, USA). Match tolerances for mass were set to 10 ppm and the cut-off for the scores was set at 70. In addition, the isotopic pattern had to match the predicted isotope pattern with a score of 70 % or higher. A feature had to

be present in at least two out of three replicates of at least one sample group to be retained. In addition, it had to be absent in negative controls (*in vitro* samples) and blanks (urine samples). MS/MS spectra were extracted using MassHunter Qualitative Analysis 10.0 (Agilent Technologies, Santa Clara, USA). Those spectra were used together with spectra from reference standards or online databases (MassBank 2.2.4, mzCloud rcmz_230612.1) to assign confidence levels of the identification according to (Schymanski et al., 2014). If no analytical standards or experimental data were available, CFM-ID 4.0 was used for *in silico* predictions of fragmentation spectra.

For the urine samples, the same suspect list as for the *in vitro* samples was used for detection of metabolites.

2.5. Semi-quantitative analysis

To quantify those metabolites in the urine samples for which no standard was available, a semi-quantification approach based on a calibration curve of BCIPHIPP was applied consisting of seven levels (in MeOH). This calibration curve covered a concentration range of 1–200 ng/mL. The IS TCEP-d12 was added in the same concentration as for the urine samples (5 ng). For each calibration point, the ratio of the peak area of BCIPHIPP and the peak area of the IS was calculated. This ratio was plotted against the BCIPHIPP concentration, and the resulting calibration curve was then fitted using a linear model with the intercept forced through 0. The response factor (R_f) was obtained by calculating the slope of the calibration curve.

The concentration of the metabolites detected in urine for which no standard was available was calculated using the following formula:

$$C_{metabolite} = \frac{Area_m / Area_{IS}}{R_f}$$

In which $c_{metabolite}$ is the concentration of the metabolite in ng/mL, $Area_m$ the peak area of the metabolite using the $[M + H]^+$ adduct, $Area_{IS}$ the peak area of the internal standard using the $[M + H]^+$ adduct and R_f the response factor of BCIPHIPP.

If the metabolite was also detected in the procedural blank, the concentration calculated in the blank was subtracted from the calculated concentrations for the samples. Spiked urine samples were injected as quality control.Urine samples were spiked at 5, 10 and 40 ng BCIPHIPP using the same sample preparation as the workers' samples. Unspiked urine was injected to correct for levels of BCIPHIPP already present in the urine. The spiked urine samples were used to determine accuracy of the BCIPHIPP calibration for the semi-quantitative analysis.

3. Results and discussion

3.1. Experimental quality controls

For Phase I biotransformation, phenacetin was used as a positive control. The formation of two established metabolites (Hinson, 1983; Christia et al., 2019) was confirmed: N-(4-hydroxyphenyl)-acetamide (phenacetin-M1) and N-(4-ethoxy-2-hydroxyphenyl)-acetamide (phenacetin-M2). Chromatograms and MS/MS spectra of phenacetin and its metabolites can be found in the Supplementary Information (SI, Fig. SI-1-3). Identification of metabolites was confirmed by comparing obtained MS/MS spectra with MS/MS spectra in libraries and *in silico* predicted MS/MS spectra.

For Phase II biotransformation, 4-nitrophenol was used as a positive control (Tukey & Strassburg, 2000; Gamage et al., 2006). The formation of 4-nitrophenol glucuronide and 4-nitrophenol sulfate was confirmed. Chromatograms and MS/MS spectra of 4-nitrophenol and its metabolites can be found in the SI (Figs. SI-4-7). Formation of metabolites was confirmed by comparing obtained MS/MS spectra with MS/MS spectra in libraries and *in silico* predicted MS/MS spectra.

Since in the positive controls for both Phase I and Phase II the expected metabolites were detected, it can be concluded that the experimental set-up was successful and possible lack of detection of metabolites was not due to experimental flaws.

Negative controls were used to check for false positive results. No TCIPP metabolites were found in the negative controls both for Phase I and Phase II biotransformation, indicating an absence of non-metabolic transformations for TCIPP.

3.2. TCIPP

TCIPP was detected in the positive ionization mode ($[M + H]^+$, *m/z* 327.0075, mass error −1.05 ppm) at a retention time of 11.45 min. Fig. SI-8 shows the chromatogram and MS/MS spectrum of TCIPP. The loss of one of the side chains resulted in a product ion at *m/z* 251.0001 (mass error: 0.00 ppm) which corresponds to $[C_6H_{14}Cl_2O_4P]^+$ ([BCIPP + H]$^+$). A loss of a second side chain resulted in the formation of a product ion at *m/z* 174.9920 (mass error: 0.57 ppm, $[C_3H_9ClO_4P]^+$). Lastly, the loss of all three side chains gave a product ion at *m/z* 98.9842 (mass error: 0.00 ppm, $[H_4O_4P]^+$), which agrees with the fragmentation pathway described in the literature (Quintana et al., 2008).

The identification of TCIPP in samples was confirmed by injecting an analytical standard and comparing retention times and fragmentation spectra resulting in identification at confidence level 1 (L1).

3.3. Phase I metabolism

Incubation of TCIPP with HLMs led to the formation of five Phase I metabolites. All the (tentatively) identified Phase I metabolites were detected in positive ionization mode ($[M + H]^+$) and were found in all relevant replicates. Table 1 displays identified metabolites with the corresponding confidence levels as proposed by Schymanski et al., 2014. All metabolites displayed in Table 1 meet the requirements listed in section 2.4.

3.3.1. BCIPP

Hydrolysis at the organophosphate moiety of TCIPP can lead to loss of one of the side chains of TCIPP resulting in formation of BCIPP. This metabolite was detected in positive ionization mode ($[M + H]^+$) and eluted at 2.7 min with *m/z* 251.0006 (mass error: 2.18 ppm). The loss of one of the side chains of BCIPP resulted in the product ion at *m/z* 174.9930 (mass error: 5.14 ppm, $[C_3H_9ClO_4P]^+$), while loss of both side chains gave the product ion at *m/z* 98.9847 (mass error: 5.05 ppm, $[H_4O_4P]^+$). This fragmentation pattern is in line with that described in literature (Dolios et al., 2019). Fig. SI-9 shows the chromatogram and the MS/MS spectrum of BCIPP. An analytical standard of BCIPP was injected to confirm the retention time and the fragmentation spectra obtained in samples. Therefore, BCIPP was identified in HLM samples at L1.

When plotting the response ratio (peak area of metabolite divided by peak area of the internal standard TCEP-d12) against the time of incubation, a slight increase in relative abundance of BCIPP was observed during the whole duration of the experiment. Fig. 2 shows the time trends of all metabolites during the experiment.

3.3.2. BCIPHIPP

The replacement of one of the chlorine atoms of TCIPP by a hydroxy group led to the formation of BCIPHIPP, which eluted at 8.32 min with *m/z* 309.0415 (mass error: −0.87) as protonated molecular ion. The loss of the hydroxylated side chain, leaving the two side chains with the chlorine atom, led to the formation of a product ion with *m/z* 250.9998 (mass error: −1.20 ppm, $[C_6H_{14}Cl_2O_4P]^+$) which is [BCIPP + H]$^+$. The additional loss of one of the side chains resulted in a product ion at *m/z* 174.9919 (mass error: −1.14 ppm, $[C_3H_9ClO_4P]^+$). The loss of the last remaining side chain gave a product ion at *m/z* 98.9845 (mass error: 3.03 ppm, $[H_4O_4P]^+$). Fig. SI-10 displays the chromatogram and MS/MS spectrum of BCIPHIPP in HLM samples. The identification of BCIPHIPP

Table 1
Summary of tris (1-chloro-2-propyl) phosphate (TCIPP) and all tentatively identified metabolites. Confidence levels, retention times (RT), measured *m/z* of the precursor ion, mass errors, tentative formulas and the *m/z* values of the diagnostic product ions are displayed.

Metabolite ID	Confidence level	RT (min)	Precursor ion Measured *m/z*	Mass error (ppm)	Molecular Formula	Diagnostic product ion (MS/MS) *m/z*
TCIPP (parent compound)	L1	11.45	327.0075	−1.05	$C_9H_{18}Cl_3O_4P$	251.0001 174.9920 98.9842
BCIPP	L1	2.77	251.0006	2.18	$C_6H_{13}Cl_2O_4P$	174.9930 98.9847
BCIPHIPP	L1	8.32	309.0415	−0.87	$C_9H_{19}Cl_2O_5P$	250.9998 174.9919 98.9845
TCIPP-M1	L3	5.36	323.0207	−1.70	$C_9H_{17}Cl_2O_6P$	247.0133 171.0042 152.9938 98.9845
TCIPP-M2	L3	8.84	307.0259	2.03	$C_9H_{17}Cl_2O_5P$	231.0183 155.0106 98.9848
TCIPP-M3	L3	9.12	343.0023	−2.12	$C_9H_{18}Cl_3O_5P$	266.9952 190.9864 174.9915 98.9842

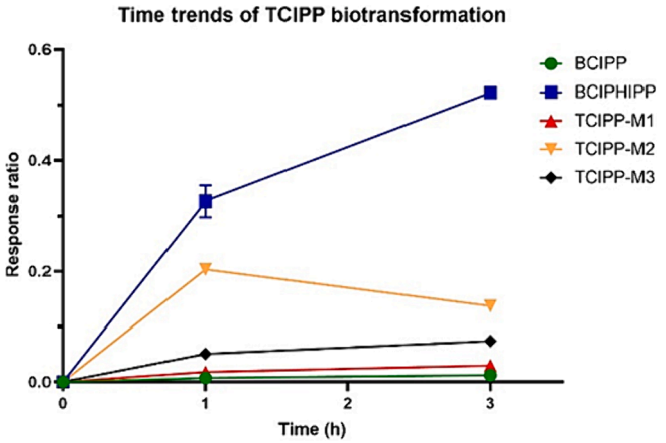

Fig. 2. Time trend of tris (1-chloro-2-propyl) phosphate (TCIPP) biotransformation. On the y-axis the response ratio (area metabolite/area internal standard) is displayed, the x-axis shows the incubation time. Time trends of five detected metabolites are shown namely 1-hydroxy-2-propyl bis (1-chloro-2-propyl) phosphate (BCIPHIPP), bis (1-chloro-2-propyl) hydrogen phosphate (BCIPP), carboxyethyl bis (1-chloro-2-propyl) phosphate (TCIPP-M1), bis (1-chloropropan-2-yl) (-oxopropan-2-yl) phosphate (TCIPP-M2) and 1-chloro-3-hydroxypropan-2-yl bis (1-chloropropan-2-yl) phosphate (TCIPP-M3). All time points consist of three replicates. Error bars are plotted but are not always visible due to the small size. Error bars represent the standard deviation of three replicates at each time point for each metabolite.

in samples was confirmed by injecting an analytical standard and comparing retention times and obtained MS/MS spectra. This resulted in identification of BCIPHIPP in HLM samples at L1.

When plotting the response ratio versus time (Fig. 2), a substantial increase in BCIPHIPP abundance can be seen during the whole incubation time.

3.3.3. TCIPP-M1

Carboxylation of one of the carbons containing a chlorine atom of TCIPP resulted in the formation of TCIPP-M1. This metabolite was detected in positive ionization mode ($[M + H]^+$) and eluted at 5.36 min with *m/z* 323.0207 (mass error:-1.70 ppm). The loss of one of the side chains with chlorine led to the formation of a production ion at *m/z* 247.0133 (mass error: 0.00 ppm, $[C_6H_{13}ClO_6P]^+$). The additional loss of the second chain containing a chlorine atom resulted in a product ion at *m/z* 171.0042 (mass error: −6.41 ppm, $[C_3H_8O_6P]^+$) leaving only the carboxylated side chain attached to the phosphate group. Additional loss of the hydroxy group attached to the phosphate group resulted in the formation of a product ion at *m/z* 152.9938 (mass error: 5.88 ppm, $[C_3H_6O_5P]^+$). The loss of the last side chain formed a product ion at *m/z* 98.9845 (mass error: 3.03 ppm, $[H_4O_4P]^+$). Fig. 3 shows the chromatogram and fragmentation spectrum of TCIPP-M1 in a Phase I sample.

Since no standards or spectra in databases and libraries were available for TCIPP-M1, the obtained MS/MS spectra were compared with *in silico* predicted fragmentation spectra. This led to the identification of TCIPP-M1 at L3. Fig. 2 shows a slight increase of the relative abundance of TCIPP-M1 throughout the whole incubation time.

3.3.4. TCIPP-M2

The replacement of a chlorine atom of TCIPP by an aldehyde function led to the formation of TCIPP-M2. This metabolite was detected in positive ionization mode ($[M + H]^+$) and eluted at 8.84 min with *m/z* 307.0259 (mass error: 2.03 ppm). The loss of one of the side chains containing a chlorine atom resulted in the product ion at *m/z* 231.0183 (mass error: 0.00 ppm, $[C_6H_{13}ClO_5P]^+$), while the loss of the additional side chain containing a chlorine atom resulted in the product ion at *m/z* 155.0106 (mass error: 1.94 ppm, $[C_3H_8O_5P]^+$). The product ion with *m/z* 98.9848 (mass error: 6.06 ppm, $[H_4O_4P]^+$) resulted from the loss of all three side chains. Since no analytical standard for this compound was available, the obtained MS/MS spectra of the samples were compared with *in silico* predicted fragmentation spectra which led to identification of TCIPP-M2 at confidence level 3. The chromatogram and MS/MS spectrum of TCIPP-M2 can be found in Fig. 4. When plotting the response ratio against the time, an increase in the relative area of TCIPP-M2 could be seen during the first hour of the incubation (Fig. 2). However, between 1 and 3 h, a decrease in abundance of TCIPP-M2 was observed, indicating that TCIPP-M2 is likely an intermediate product that is initially formed as a metabolite, but is then converted to other TCIPP metabolites (such as TCIPP-M1).

3.3.5. TCIPP-M3

Oxidation of one of the methyl groups on one of the side chains of TCIPP led to the formation of another metabolite, TCIPP-M3. This metabolite was detected in positive ionization mode ($[M + H]^+$) and eluted at 9.12 min with *m/z* 343.0023 (mass error: −2.12 ppm). The loss of one of the non-hydroxylated side chains led to a product ion with *m/z* 266.9952 (mass error: 0.75 ppm, $[C_6H_{14}Cl_2O_5P]^+$), while the loss of both non-hydroxylated side chains resulted in a product ion at *m/z*

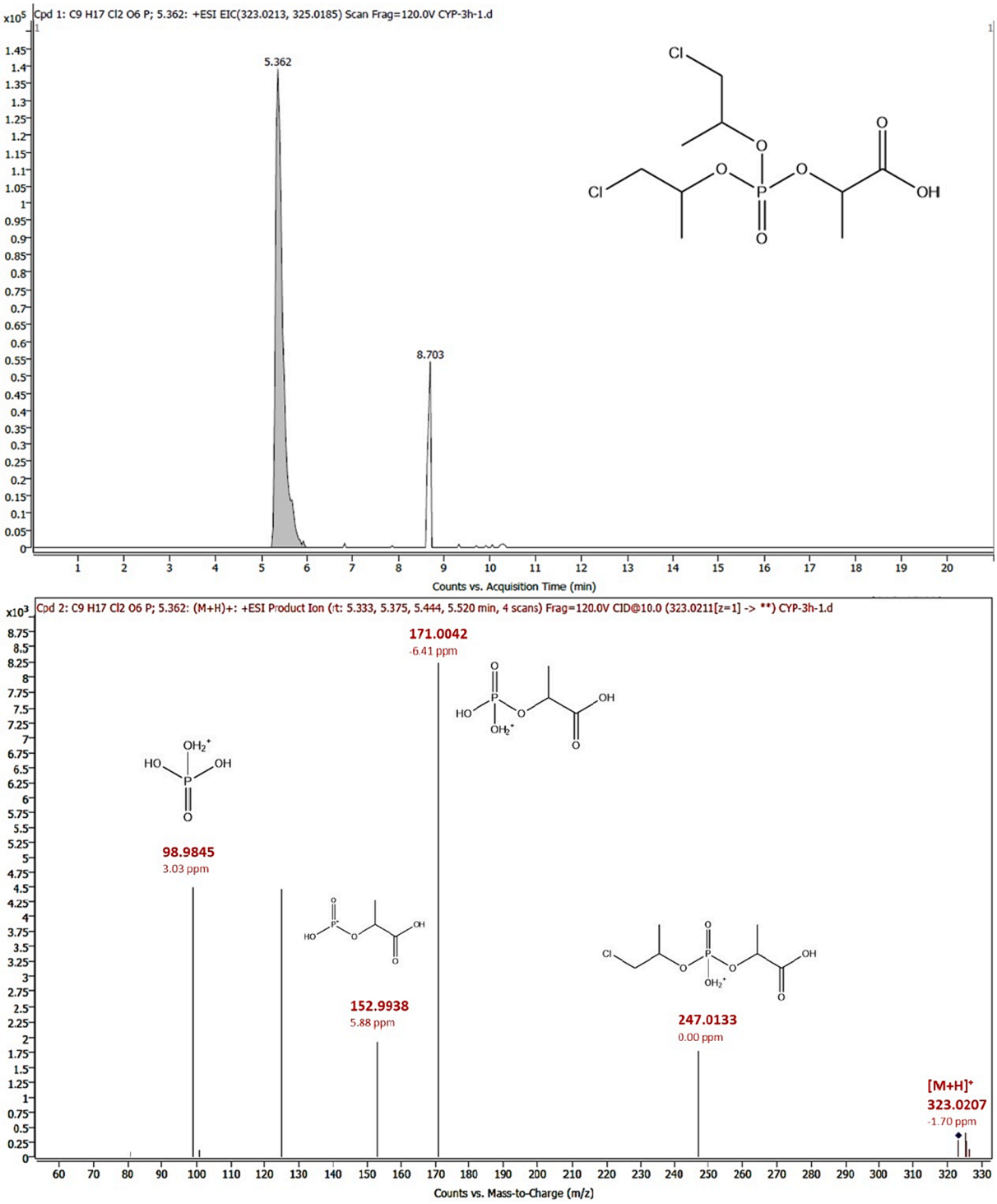

Fig. 3. Chromatogram $[M + H]^+$ and molecular structure (top) and MS/MS spectrum of carboxy ethyl bis (1-chloro-2-propyl) phosphate (TCIPP-M1) at 10 eV (bottom) in HLM samples. Found *m/z* values, mass errors and proposed structures are indicated.

190.9864 (mass error: −3.67 ppm, $[C_3H_9ClO_5P]^+$). If instead of the second non-hydroxylated side chain, the hydroxylated side chain was lost, a product ion at *m/z* 174.9915 (mass error: −3.43 ppm, $[C_3H_9ClO_4P]^+$) was formed. Moreover, the product ion at *m/z* 98.9842 (mass error: 0.00 ppm, $[H_4O_4P]^+$) is the result of the loss of all three side chains. Based on fragmentation spectra, it cannot be said with certainty on what exact position the hydroxy group is placed. It can be positioned on the ethyl group as well as on the methylene group to which the chlorine molecule is attached. Because of lack of an analytical standard or fragmentation spectra in libraries and databases for this compound, obtained MS/MS spectra of samples were compared with *in silico* predicted fragmentation spectra leading to confirmation at L3. Fig. 5 shows the chromatogram and MS/MS spectrum of TCIPP-M3 of an HLM sample. When plotting the response ratio against the time, a slight increase of TCIPP-M3 could be seen from the start of the incubation until the end of incubation (Fig. 2).

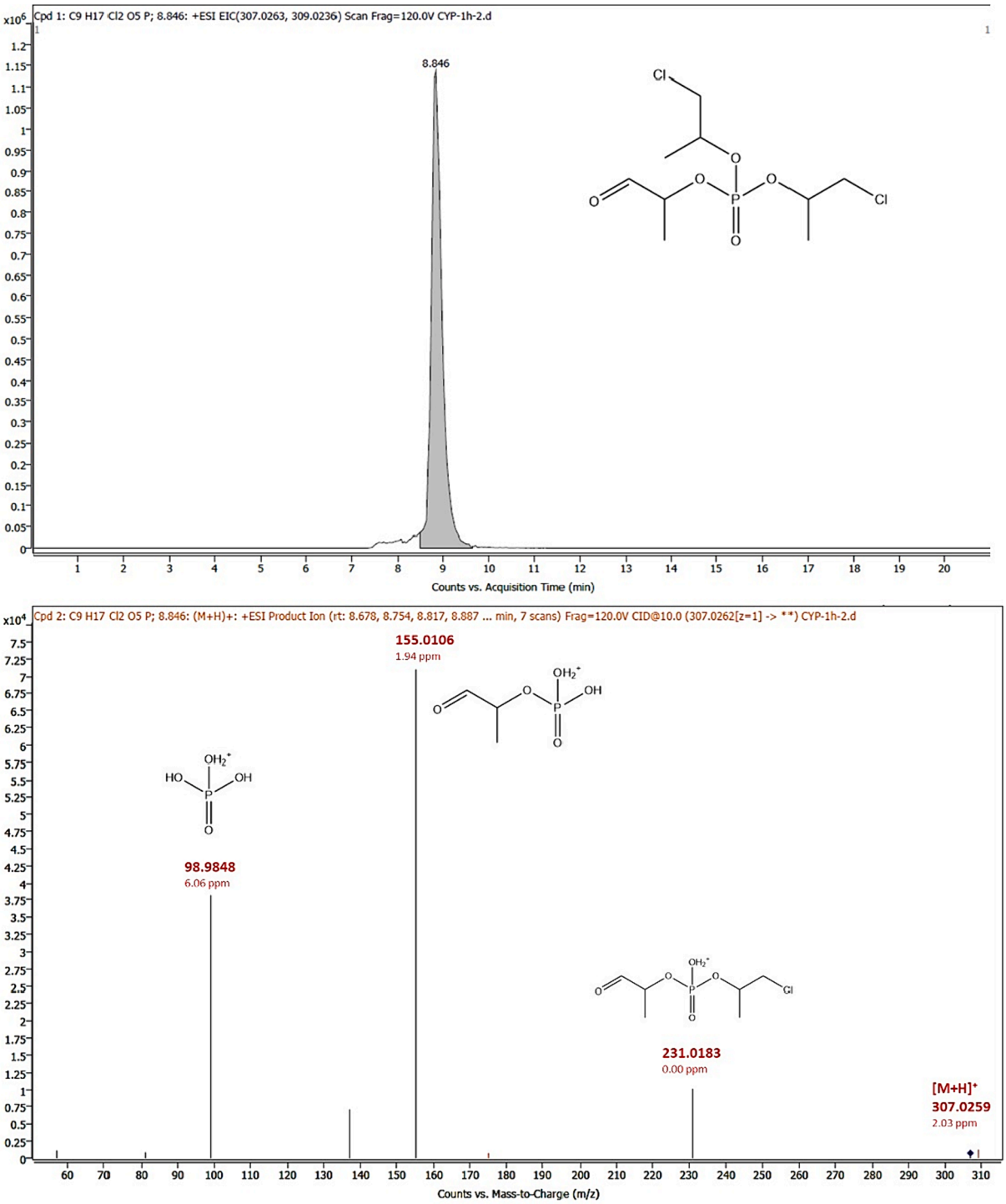

Fig. 4. Chromatogram $[M + H]^+$ and molecular structure (top) and MS/MS spectrum at 10 eV (bottom) of product bis (1-chloropropan-2-yl) (-oxopropan-2-yl) phosphate (TCIPP-M2) in HLM samples. Found *m/z* values, mass errors and proposed structures are indicated.

3.4. Phase II metabolism

All metabolites that were detected in the Phase I samples, could also be detected in the Phase II samples. Although Abdallah et al., 2015 and Wan et al., 2017 identified a glutathione product, no Phase II metabolites were found in this study. Moreover, the absence of formation of a glutathione product can be because in this study S9 fractions were not used to investigate biotransformation.

3.5. In vitro biotransformation of TCIPP

The Phase I and Phase II biotransformation of TCIPP were examined *in vitro* using HLMs and HLCYT. In line with other studies, BCIPP and BCIPHIPP were detected as metabolites of TCIPP (Van den Eede et al., 2013; Abdallah et al., 2015; Van den Eede et al., 2016). In addition, the *in vitro* formation of TCIPP-M1 and TCIPP-M3 was confirmed (Abdallah et al., 2015; Van den Eede et al., 2016; Wan et al., 2017). This study has also identified the *in vitro* formation of the intermediate product TCIPP-M2. This intermediate product was formed as metabolite of TCIPP but

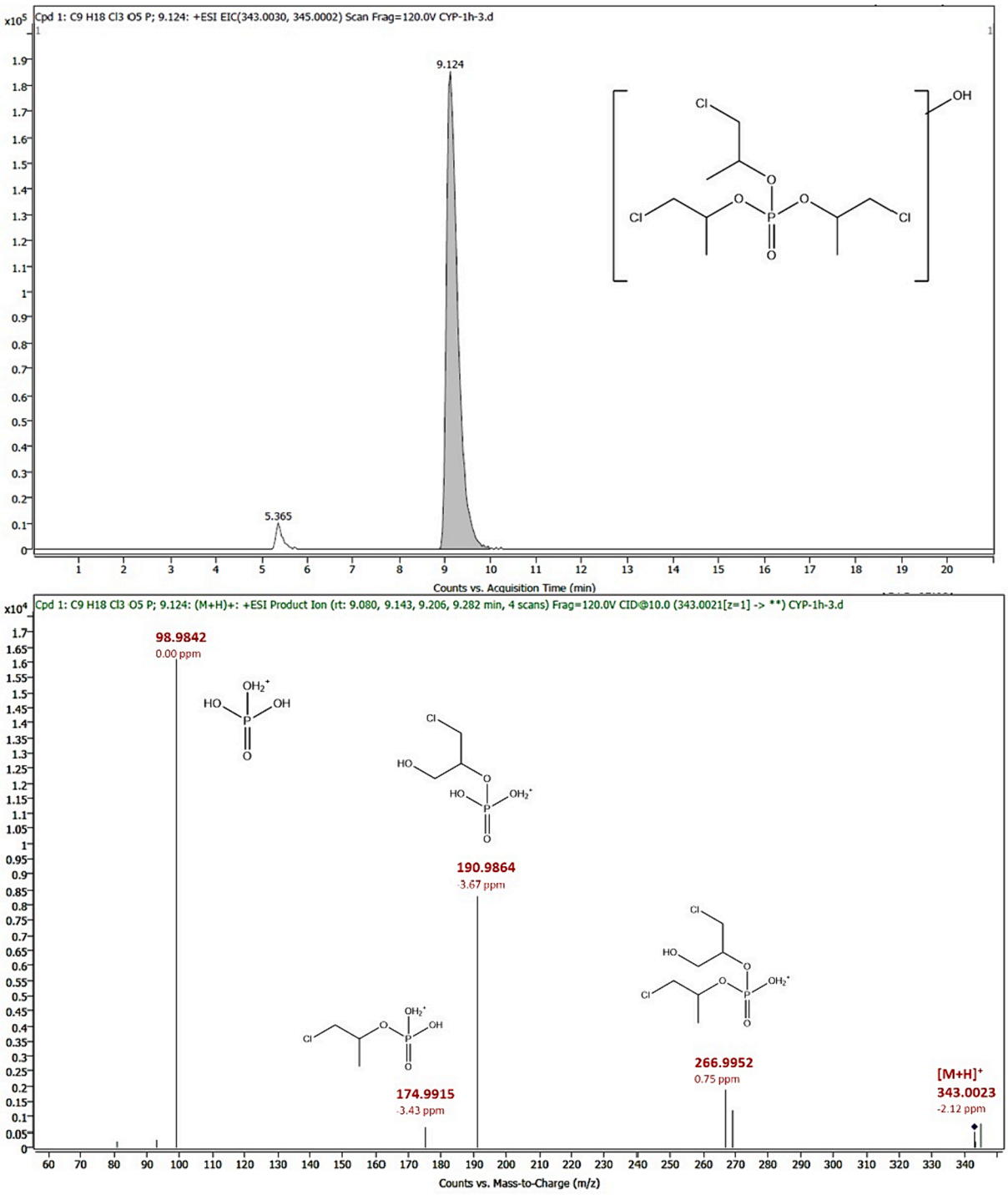

Fig. 5. Chromatogram $[M + H]^+$ (top) and MS/MS spectrum at 10 eV (bottom) of 1-chloro-3-hydroxypropan-2-yl bis (1-chloropropan-2-yl) phosphate (TCIPP-M3) in an HLM sample. Found *m/z* values, mass errors and proposed structures are indicated.

was subsequently metabolized to other TCIPP metabolites. To our knowledge, this is the first time that the formation of this intermediate product has been reported. These results allowed the identification of a biotransformation pathway of TCIPP (Fig. 6). TCIPP can be directly converted to BCIPHIPP, BCIPP, TCIPP-M2 and TCIPP-M3. TCIPP-M2 is an intermediate product that can be converted to TCIPP-M1 and BCIPP. Based on the relative areas, BCIPHIPP was the major formed metabolite, followed by TCIPP-M2, TCIPP-M3 and TCIPP-M1, while BCIPP was formed to a lesser extent. To our knowledge, the five identified metabolites cannot derive from any other parent compound than TCIPP. In addition, literature does not report the use of any of these metabolites itself as flame retardants or in any other application.

3.6. Urine samples

To investigate the *in vivo* biotransformation of TCIPP, 56 urine samples from people occupationally exposed to TCIPP were obtained. First, these samples were quantified to determine the ones with the highest TCIPP exposure (as described in section 2.2, data not shown). These results will be shared in a future manuscript. Based on the BCIPP

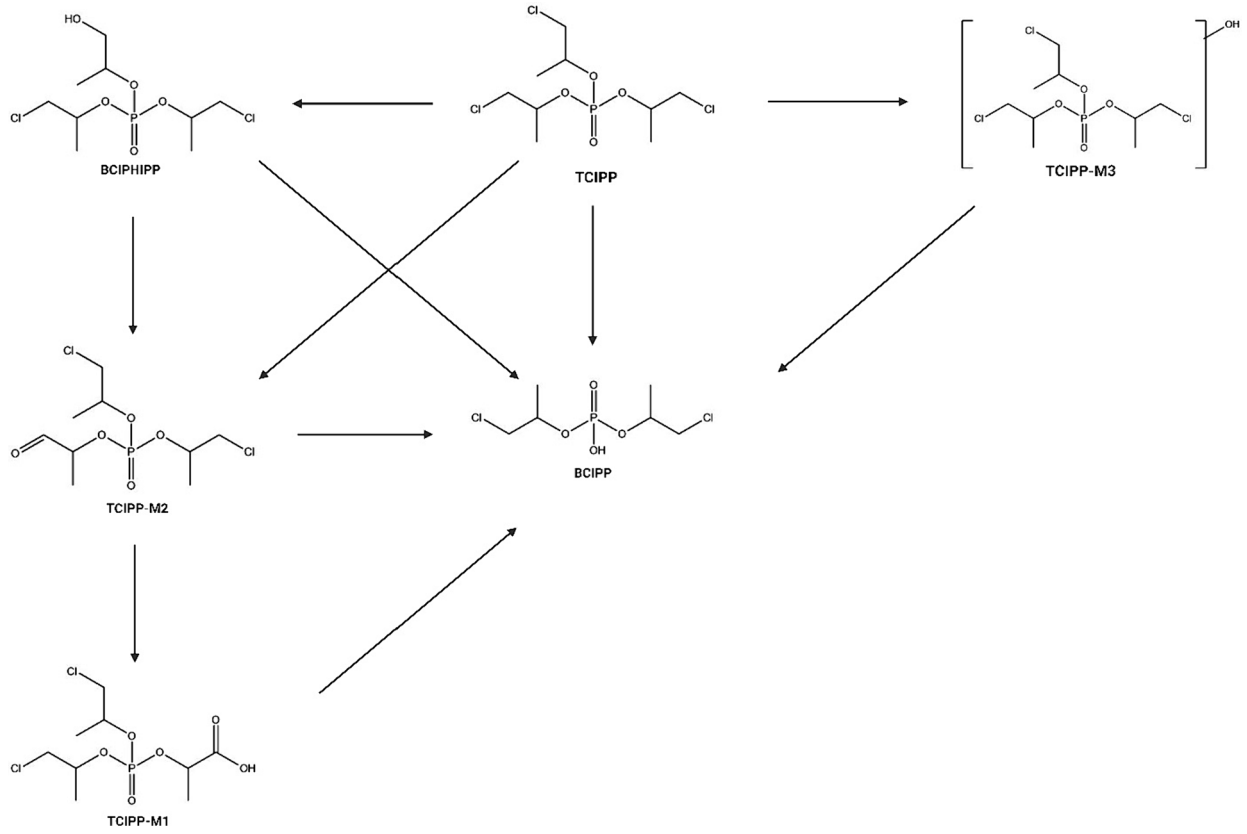

Fig. 6. Proposed biotransformation pathway of tris (1-chloro-2-propyl) phosphate (TCIPP) including the metabolites 1-hydroxy-2-propyl bis (1-chloro-2-propyl) phosphate (BCIPHIPP), bis (1-chloro-2-propyl) hydrogen phosphate (BCIPP), bis (1-chloro-2-propyl) phosphate (TCIPP-M1), bis (1-chloropropan-2-yl) (-oxopropan-2-yl) phosphate (TCIPP-M2) and 1-chloro-3-hydroxypropan-2-yl bis (1-chloropropan-2-yl) phosphate (TCIPP-M3).

and BCIPHIPP levels found in the targeted analysis, apart from blanks and spiked urine samples, 14 samples were selected for suspect screening.

BCIPHIPP was detected in all selected samples. Obtained fragmentation spectra were compared with fragmentation spectra of an analytical standard. This resulted in matches in retention time and product ions, which indicates confidence level 1. Chromatograms and spectra for all metabolites detected in the urine samples can be found in the SI (Fig. SI-11-17).

BCIPP was detected in 2 out of 14 samples. No MS/MS spectra could be obtained for this compound in urine samples, due to low concentrations and poor intrinsic response. However, the retention time of BCIPP in the sample could be confirmed with the retention time of an injected standard resulting in level 2c confidence (Roggeman et al., 2022).

TCIPP-M1 was detected in 10 out of 14 samples. Since no standard was available for this compound, the obtained MS/MS spectra were compared with *in silico* predicted spectra. Since matches were found for the obtained spectra for urine samples with spectra from *in vitro* experiments and predicted spectra and retention times matched in HLM and urine samples, this led to confidence level 3.

TCIPP-M3 was detected in all 14 samples. Because of the lack of an analytical standard for this compound, obtained MS/MS spectra were compared with *in silico* predicted spectra. Matches were found for the obtained spectra in urine with spectra from HLM samples and predicted spectra were found, resulting in a level 3 confidence.

TCIPP-M2 was not detected in any of the urine samples. This aldehyde compound was identified as an intermediate product during the *in vitro* experiments. In the human body, TCIPP-M2 might thus be converted rapidly to other metabolites, resulting in concentrations in the urine that are too low to be detected in a suspect screening using LC-QTOF-MS analysis. In addition, this aldehyde is a reactive product and could therefore be degraded during the sample preparation.

Using urine from an occupationally exposed population, the *in vivo* formation of four TCIPP metabolites was confirmed. As expected, BCIPP and BCIPHIPP were detected in urine (Araki et al., 2018; Phillips et al., 2018; Luo et al., 2021). However, to the best of our knowledge this is the first time TCIPP-M1 and TCIPP-M3 have been detected in human urine. TCIPP-M2, which was detected during the *in vitro* experiment, was not detected in human urine, probably because, as mentioned before, this metabolite was identified as an intermediate product. Apart from the metabolites that were already detected during the *in vitro* experiment, no additional metabolites were identified in the urine samples.

3.7. Semi-quantitative analysis

Since no standards were available for TCIPP-M1 and TCIPP-M3, a semi-quantitative approach based on a calibration series of BCIPHIPP was used to estimate the concentrations of these two compounds in the 14 urine samples injected for suspect screening. The obtained calibration curve for BCIPHIPP can be found in the SI (Fig. SI-18). Spiked urine samples (5, 10 and 40 ng BCIPHIPP), using the same sample preparation as the workers' samples, were included as quality control. Results for these samples showed that the BCIPHIPP concentration resulting from the calibration curve on the QTOF overestimated the BCIPHIPP levels showing levels 180 % of the theoretical value due to a strong matrix effect (signal enhancement). Therefore, the found concentrations were corrected by 0.55 to account for such matrix effects. The median concentrations in the investigated samples were 89.0 ng/mL (range 10.6–591.4 ng/mL) for BCIPHIPP, 4.40 ng/mL (0.12–26.4 ng/mL) for TCIPP-M3, and 2.53 ng/mL (0.06–14.7 ng/mL) for TCIPP-M1. The concentrations of metabolites in each sample can be found in Table S1.

The calculated concentration ranges align with the trend in response ratios found in the *in vitro* experiments (Fig. 2) in which BCIPHIPP was formed to the largest extent, followed by TCIPP-M2, TCIPP-M3 and lastly TCIPP-M1.

BCIPHIPP concentrations found in this study are higher than those found in the general population (Van den Eede et al., 2015; Hammel et al., 2016; Bastiaensen et al., 2018; Xu et al., 2019). However, the population in this study was occupationally exposed meaning that higher concentrations can be expected. Bello et al., 2018 used a population occupationally exposed to TCIPP and found BCIPHIPP concentrations in the same order of magnitude with a geometric mean of 88.8 ng/mL (range 5.2–703 ng/mL). TCIPP-M1 and TCIPP-M3 have not been reported as metabolites in urine before and therefore no comparisons with literature can be made. Compared with BCIPHIPP, concentrations of these two metabolites are significantly lower, but it might still be worth exploring the possibilities of a quantitative method for these compounds to determine their potential in estimating TCIPP exposure. In addition, even if the metabolites occur in low concentrations, their toxic potential is still unknown and should be elucidated. Even though a targeted method based on triple quadrupole MS is usually more sensitive than the screening approach applied here, it should be kept in mind that in the general population concentrations of these metabolites are probably lower and therefore could be below detection limits. In addition, to develop a targeted method in the future, analytical standards of high purity of these compounds will be needed, likely obtained by custom synthesis, since no commercial standards are available.

4. Conclusions

This study identified five Phase I TCIPP metabolites *in vitro* including one intermediate product, TCIPP-M2, that has not yet been reported in literature. In addition, four of these metabolites were identified in urine from people occupationally exposed to TCIPP. Two of those metabolites, namely TCIPP-M1 and TCIPP-M3, were identified for the first time in human urine. It is remarkable that BCIPP, an established biomarker for TCIPP, was only detected in 2 out of 14 urine samples, while TCIPP-M1 and TCIPP-M3 were detected in 10 and 14 urine samples, respectively. The findings in urine are in agreement with the *in vitro* results. This observation shows that while BCIPP is now used as a biomarker of TCIPP exposure, it might be worth exploring the incorporation of TCIPP-M1 and/or TCIPP-M3 as biomarkers for TCIPP exposure in future biomonitoring. The obtained data in this study contribute to a more reliable assessment of human exposure to TCIPP by proposing TCIPP-M1 and TCIPP-M3 as potential additional biomarkers next to BCIPP and BCIPHIPP.

Declaration of competing interest

The authors declare that they have no known competing financial interests or personal relationships that could have appeared to influence the work reported in this paper.

Data availability

Data will be made available on request.

Acknowledgements

We thank the workers who voluntarily donated their urine to this project. This work was supported by the Interuniversity Special Research Fund from Flanders (iBOF Grant BOFIBO2021001102, Flexigut project) and the Exposome Centre of Excellence of the University of Antwerp (BOF grant, Antigoon database number 41222). L. Belova and M. Roggeman acknowledge funding through Research Foundation Flanders (FWO) fellowships (11G1821N and 1133223N respectively). Authors from the University of Santiago de Compostela further acknowledge funding through Consellería de Cultura de Galicia, Educación e Universidades (ref. ED481A-2020/258 & ED431C 2021/06) and Spanish Agencia Estatal de Investigación – MCIN/AEI/10.13039/501100011033 (ref. PID2020-117686RB-C32). A. Klimowska acknowledges a fellowship (BPN/BEK/2021/1/00132/U/00001) funded by the National Agency for Academic Exchange (NAWA) under the Bekker Programme (2021).

Appendix A. Supplementary data

Supplementary data to this article can be found online at https://doi.org/10.1016/j.crtox.2024.100164.

References

Abdallah, M.A.E., Zhang, J., Pawar, G., Viant, M.R., Chipman, J.K., D'Silva, K., Bromirski, M., Harrad, S., 2015. High-resolution mass spectrometry provides novel insights into products of human metabolism of organophosphate and brominated flame retardants. Anal. Bioanal. Chem. 407 (7), 1871–1883. https://doi.org/10.1007/s00216-015-8466-z.

Araki, A., Saito, I., Kanazawa, A., Morimoto, K., Nakayama, K., Shibata, E., Tanaka, M., Takigawa, T., Yoshimura, T., Chikara, H., Saijo, Y., Kishi, R., 2014. Phosphorus flame retardants in indoor dust and their relation to asthma and allergies of inhabitants. Indoor Air 24 (1), 3–15. https://doi.org/10.1111/ina.12054.

Araki, A., Bastiaensen, M., Ait Bamai, Y., Van den Eede, N., Kawai, T., Tsuboi, T., Ketema, R.M., Covaci, A., Kishi, R., 2018. Associations between allergic symptoms and phosphate flame retardants in dust and their urinary metabolites among school children. Environ. Int. 119 (July), 438–446. https://doi.org/10.1016/j.envint.2018.07.018.

Bastiaensen, M., Xu, F., Been, F., Van den Eede, N., Covaci, A., 2018. Simultaneous determination of 14 urinary biomarkers of exposure to organophosphate flame retardants and plasticizers by LC-MS/MS. Anal. Bioanal. Chem. 410 (30), 7871–7880. https://doi.org/10.1007/s00216-018-1402-2.

Bello, A., Carignan, C.C., Xue, Y., Stapleton, H.M., Bello, D., 2018. Exposure to organophosphate flame retardants in spray polyurethane foam applicators: role of dermal exposure. Environ. Int. 113 (November 2017), 55–65. https://doi.org/10.1016/j.envint.2018.01.020.

Beser, M.I., Pardo, O., Beltrán, J., Yusà, V., 2019. Determination of 21 perfluoroalkyl substances and organophosphorus compounds in breast milk by liquid chromatography coupled to orbitrap high-resolution mass spectrometry. Anal. Chim. Acta 1049, 123–132. https://doi.org/10.1016/j.aca.2018.10.033.

Blum, A., Behl, M., Birnbaum, L.S., Diamond, M.L., Phillips, A., Singla, V., Sipes, N.S., Stapleton, H.M., Venier, M., 2019. Organophosphate ester flame retardants: are they a regrettable substitution for polybrominated diphenyl ethers? Environ. Sci. Technol. Lett. 6 (11), 638–649. https://doi.org/10.1021/acs.estlett.9b00582.

Chen, X., Zhao, X., Shi, Z., 2021. Organophosphorus flame retardants in breast milk from Beijing, China: occurrence, nursing infant's exposure and risk assessment. Sci. Total Environ. 771, 145404 https://doi.org/10.1016/j.scitotenv.2021.145404.

Christia, C., Tang, B., Yin, S.S., Luo, X.J., Mai, B.X., Poma, G., Covaci, A., 2019. Simultaneous determination of legacy and emerging organophosphorus flame retardants and plasticizers in indoor dust using liquid and gas chromatography–tandem mass spectrometry: method development, validation, and application. Anal. Bioanal. Chem. 411 (26), 7015–7025. https://doi.org/10.1007/s00216-019-02078-5.

Christia, C., da Silva, K.M., Poma, G., van Nuijs, A.L.N., Covaci, A., 2021. In vitro phase I metabolism of newly identified plasticizers using human liver microsomes combined with high resolution mass spectrometry and based on non-targeted and suspect screening workflows. Toxicol. Lett. 356, 33–40. https://doi.org/10.1016/j.toxlet.2021.12.005.

de la Torre, A., Navarro, I., Sanz, P., de los Ángeles Martínez, M., 2020. Organophosphate compounds, polybrominated diphenyl ethers and novel brominated flame retardants in European indoor house dust: use, evidence for replacements and assessment of human exposure. J. Hazard. Mater. 382 (August 2019), 121009 https://doi.org/10.1016/j.jhazmat.2019.121009.

Dolios, G., Patel, D., Arora, M., Andra, S.S., 2019. Mass defect filtering for suspect screening of halogenated environmental chemicals: a case study of chlorinated organophosphate flame retardants. Rapid Commun. Mass Spectrom. 33 (5), 503–519. https://doi.org/10.1002/rcm.8370.

EHC, 1998. Environmental Health Criteria 209: Flame retardants: tris (chloropropyl) phosphate and tris (2-chloroethyl) phosphate.

Estill, C.F., Slone, J., Mayer, A.C., Phillips, K., Lu, J., Chen, I.C., Christianson, A., Streicher, R., Guardia, M.J.L., Jayatilaka, N., Ospina, M., Calafat, A.M., 2019. Assessment of spray polyurethane foam worker exposure to organophosphate flame retardants through measures in air, hand wipes, and urine. J. Occup. Environ. Hyg. 16 (7), 477–488. https://doi.org/10.1080/15459624.2019.1609004.

European Chemicals Agency, E., 2018. Screening Report. An assessment of whether the use of TCEP, TCPP and TDCP in articles should be restricted. April, 1–68. https://echa.europa.eu/documents/10162/13641/screening_report_tcep_tcpp_td-cp_en.pdf/e0960aa7-f703-499c-24ff-fba627060698.

European Chemicals Agency, E., 2023. Regulatory strategy for flame retardants (Issue March). https://doi.org/10.2823/854233.

Farhat, A., Crump, D., Chiu, S., Williams, K.L., Letcher, R.J., Gauthier, L.T., Kennedy, S. W., 2013. In ovo effects of two organophosphate flame Retardants-TCPP and TDCPP-on pipping success, development, mRNA expression, and thyroid hormone levels in chicken embryos. Toxicol. Sci. 134 (1), 92–102. https://doi.org/10.1093/toxsci/kft100.

Gamage, N., Barnett, A., Hempel, N., Duggleby, R.G., Windmill, K.F., Martin, J.L., McManus, M.E., 2006. Human sulfotransferases and their role in chemical metabolism. Toxicol. Sci. 90 (1), 5–22. https://doi.org/10.1093/toxsci/kfj061.

Gbadamosi, M.R., Abdallah, M.A.E., Harrad, S., 2022. Organophosphate esters in UK diet; exposure and risk assessment. Sci. Total Environ. 849 (September), 158368 https://doi.org/10.1016/j.scitotenv.2022.158368.

Gys, C., Kovačič, A., Huber, C., Lai, F.Y., Heath, E., Covaci, A., 2018. Suspect and untargeted screening of bisphenol S metabolites produced by in vitro human liver metabolism. Toxicol. Lett. 295 (May), 115–123. https://doi.org/10.1016/j.toxlet.2018.05.034.

Hammel, S.C., Hoffman, K., Webster, T.F., Anderson, K.A., Stapleton, H.M., 2016. Measuring personal exposure to organophosphate flame Retardants using silicone wristbands and hand wipes. Environ. Sci. Tech. 50 (8), 4483–4491. https://doi.org/10.1021/acs.est.6b00030.

Hammel, S.C., Hoffman, K., Lorenzo, A.M., Chen, A., Phillips, A.L., Butt, C.M., Sosa, J.A., Webster, T.F., Stapleton, H.M., 2017. Associations between flame retardant applications in furniture foam, house dust levels, and residents' serum levels. Environ. Int. 107 (July), 181–189. https://doi.org/10.1016/j.envint.2017.07.015.

He, M.J., Lu, J.F., Ma, J.Y., Wang, H., Du, X.F., 2018. Organophosphate esters and phthalate esters in human hair from rural and urban areas, Chongqing, China: concentrations, composition profiles and sources in comparison to street dust. Environ. Pollut. 237, 143–153. https://doi.org/10.1016/j.envpol.2018.02.040.

Hinson, J.A., 1983. Reactive metabolites of phenacetin and acetaminophen: a review. Environ. Health Perspect. 49, 71–79. https://doi.org/10.1289/ehp.834971.

Hou, M., Shi, Y., Jin, Q., Cai, Y., 2020. Organophosphate esters and their metabolites in paired human whole blood, serum, and urine as biomarkers of exposure. Environ. Int. 139 (October 2019), 105698 https://doi.org/10.1016/j.envint.2020.105698.

Hou, M., Fang, J., Shi, Y., Tang, S., Dong, H., Liu, Y., Deng, F., Giesy, J.P., Godri Pollitt, K.J., Cai, Y., Shi, X., 2021. Exposure to organophosphate esters in elderly people: relationships of OPE body burdens with indoor air and dust concentrations and food consumption. Environ. Int. 157, 106803 https://doi.org/10.1016/j.envint.2021.106803.

Hou, R., Xu, Y., Wang, Z., 2016. Review of OPFRs in animals and humans: absorption, bioaccumulation, metabolism, and internal exposure research. Chemosphere 153, 78–90. https://doi.org/10.1016/j.chemosphere.2016.03.003.

Li, Y., Li, D., Chen, J., Zhang, S., Fu, Y., Wang, N., Liu, Y., Zhang, B., 2020. Presence of organophosphate esters in plasma of patients with hypertension in Hubei Province, China. *Environ. Sci. Pollut. Res.* 27 (19), 24059–24069. https://doi.org/10.1007/s11356-020-08563-0.

Li, F., Wang, L., Ji, C., Wu, H., Zhao, J., Tang, J., 2017. Toxicological effects of tris(2-chloropropyl) phosphate in human hepatic cells. Chemosphere 187, 88–96. https://doi.org/10.1016/j.chemosphere.2017.08.083.

Liu, L.Y., He, K., Hites, R.A., Salamova, A., 2016. Hair and nails as noninvasive Biomarkers of human exposure to brominated and organophosphate flame Retardants. Environ. Sci. Tech. 50 (6), 3065–3073. https://doi.org/10.1021/acs.est.5b05073.

Luo, D., Liu, W., Wu, W., Tao, Y., Hu, L., Wang, L., Yu, M., Zhou, A., Covaci, A., Xia, W., Xu, S., Li, Y., Mei, S., 2021. Trimester-specific effects of maternal exposure to organophosphate flame retardants on offspring size at birth: A prospective cohort study in China. J. Hazard. Mater., 406(December 2020), 124754. https://doi.org/10.1016/j.jhazmat.2020.124754.

NTP, 2023. NTP Technical Report on the Toxicology and Carcinogensis Studies of an Isometic Mixture of Tris (chloropropyl) phosphate Adminstered in Feed to Sprague Dawley Rats and B6C3F1/N Mice.

OEHHA, 2021. The proposition 65 list. 2021. https://oehha.ca.gov/proposition-65/proposition-65-list.

Phillips, A.L., Hammel, S.C., Hoffman, K., Lorenzo, A.M., Chen, A., Webster, T.F., Stapleton, H.M., 2018. Children's residential exposure to organophosphate ester flame retardants and plasticizers: investigating exposure pathways in the TESIE study. Environ. Int. 116 (April), 176–185. https://doi.org/10.1016/j.envint.2018.04.013.

Piringer, O.G., Baner, A.L., 2008. Plastic Packaging: Interactions with Food and Pharmaceuticals, 2nd ed. Wiley-VCH.

Poma, G., Glynn, A., Malarvannan, G., Covaci, A., Darnerud, P.O., 2017. Dietary intake of phosphorus flame retardants (PFRs) using Swedish food market basket estimations. Food Chem. Toxicol. 100, 1–7. https://doi.org/10.1016/j.fct.2016.12.011.

Poma, G., Sales, C., Bruyland, B., Christia, C., Goscinny, S., Van Loco, J., Covaci, A., 2018. Occurrence of organophosphorus flame Retardants and plasticizers (PFRs) in belgian foodstuffs and estimation of the Dietary exposure of the adult population. Environ. Sci. Tech. 52 (4), 2331–2338. https://doi.org/10.1021/acs.est.7b06395.

Quintana, J.B., Rodil, R., Reemtsma, T., García-López, M., Rodríguez, I., 2008. Organophosphorus flame retardants and plasticizers in water and air II. analytical methodology. TrAC - Trends Anal. Chem. 27 (10), 904–915. https://doi.org/10.1016/j.trac.2008.08.004.

Roggeman, M., Belova, L., Fernández, S.F., Kim, D.H., Jeong, Y., Poma, G., Remy, S., Verheyen, V.J., Schoeters, G., van Nuijs, A.L.N., Covaci, A., 2022. Comprehensive suspect screening for the identification of contaminants of emerging concern in urine of flemish adolescents by liquid chromatography high-resolution mass spectrometry. Environ. Res. 214 (March) https://doi.org/10.1016/j.envres.2022.114105.

Schwope, A. D., Goydan, R., & Reid, R. C. (1990). Methodology for Estimating the Migration of Additives and Impurities from Polymeric Materials.

Schymanski, E.L., Jeon, J., Gulde, R., Fenner, K., Ru, M., Singer, H.P., Hollender, J., 2014. Identifying small molecules via high resolution mass spectrometry: communicating con fi dence. Environ. Sci. Tech. 48, 2097–2098. https://doi.org/10.1021/es5002105.

Tukey, R. H., & Strassburg, C. P. (2000). human UDP-G Lucuronosyltransferases : Metabolism , Expression , and Disease. 581–616.

Van den Eede, N., Maho, W., Erratico, C., Neels, H., Covaci, A., 2013. First insights in the metabolism of phosphate flame retardants and plasticizers using human liver fractions. Toxicol. Lett. 223 (1), 9–15. https://doi.org/10.1016/j.toxlet.2013.08.012.

Van den Eede, N., Heffernan, A.L., Aylward, L.L., Hobson, P., Neels, H., Mueller, J.F., Covaci, A., 2015. Age as a determinant of phosphate flame retardant exposure of the australian population and identification of novel urinary PFR metabolites. Environ. Int. 74, 1–8. https://doi.org/10.1016/j.envint.2014.09.005.

Van den Eede, N., Tomy, G., Tao, F., Halldorson, T., Harrad, S., Neels, H., Covaci, A., 2016. Kinetics of tris (1-chloro-2-propyl) phosphate (TCIPP) metabolism in human liver microsomes and serum. Chemosphere 144, 1299–1305. https://doi.org/10.1016/j.chemosphere.2015.09.049.

van der Veen, I., de Boer, J., 2012. Phosphorus flame retardants: properties, production, environmental occurrence, toxicity and analysis. Chemosphere 88 (10), 1119–1153. https://doi.org/10.1016/j.chemosphere.2012.03.067.

Vervliet, P., de Nys, S., Duca, R.C., Boonen, I., Godderis, L., Elskens, M., van Landuyt, K. L., Covaci, A., 2020. Human phase I in vitro liver metabolism of two bisphenolic diglycidyl ethers BADGE and BFDGE. Toxicol. Lett. 332 (April), 7–13. https://doi.org/10.1016/j.toxlet.2020.06.022.

Wan, W., Huang, H., Lv, J., Han, R., Zhang, S., 2017. Uptake, translocation, and Biotransformation of organophosphorus esters in wheat (Triticum aestivum L.). Environ. Sci. Tech. 51 (23), 13649–13658. https://doi.org/10.1021/acs.est.7b01758.

Wei, G.L., Li, D.Q., Zhuo, M.N., Liao, Y.S., Xie, Z.Y., Guo, T.L., Li, J.J., Zhang, S.Y., Liang, Z.Q., 2015. Organophosphorus flame retardants and plasticizers: sources, occurrence, toxicity and human exposure. Environ. Pollut. 196, 29–46. https://doi.org/10.1016/j.envpol.2014.09.012.

Xu, F., Eulaers, I., Alves, A., Papadopoulou, E., Padilla-Sanchez, J.A., Lai, F.Y., Haug, L. S., Voorspoels, S., Neels, H., Covaci, A., 2019. Human exposure pathways to organophosphate flame retardants: associations between human biomonitoring and external exposure. Environ. Int. 127 (February), 462–472. https://doi.org/10.1016/j.envint.2019.03.053.